JCTC Journal of Chemical Theory and Computation

Article

pubs.acs.org/JCTC

Partitioned EOMEA-MBPT(2): An Efficient N^5 Scaling Method for Calculation of Electron Affinities

Achintya Kumar Dutta, Jitendra Gupta, Himadri Pathak, Nayana Vaval, and Sourav Pal*

Physical Chemistry Division, CSIR-National Chemical Laboratory, Pune-411008, India

Supporting Information

ABSTRACT: We present an N^5 scaling modification to the standard EOMEA-CCSD method, based on the matrix partitioning technique and perturbative approximations. The method has lower computational scaling and smaller storage requirements than the standard EOMEA-CCSD method and, therefore, can be used to calculate electron affinities of large molecules and clusters. The performance and capabilities of the new method have been benchmarked with the standard EOMEA-CCSD method, for a test set of 20 small molecules, and the average absolute deviation is only 0.03 eV. The method is further used to investigate electron affinities of DNA and RNA nucleobases, and the results are in excellent agreement with the experimental values.

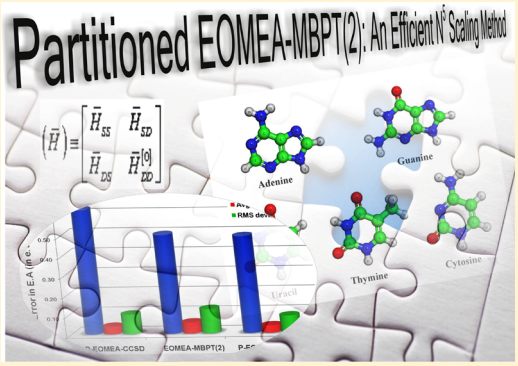

1. INTRODUCTION

Electron affinities are one of the intrinsic properties of atoms and molecules and are of interest to both theoreticians and experimentalists. In spite of its immense importance in chemistry and biology, experimental determination of electron affinities is rather complicated. The main reason behind the experimental uncertainty is the ambiguous nature of the anion formed after electron attachment. There are two alternative possibilities: valence bound (VB), which involves attachment of an additional electron to the antibonding molecular orbital, leading to significant structural change of the molecule. On the other hand, there exists an alternative possibility in polar molecules (dipole moment equal to or higher than 2.5 D), where the additional electron remains weekly bound to the molecule by charge-dipole interaction (DB),[1,2] and the structure remains almost unchanged from that of the neutral precursor. Now, energetically VB and DB can be near degenerate, and depending on the experimental condition, either of them can be formed, which makes experimental determination of electron affinity complicated. Theoretical calculations can be helpful for the reliable determination of electron affinities. The *ab initio* computation of electron affinity is also challenging, however, due to different reasons. The Hartree−Fock approximation often does not bind the excess electron or bind it very weakly.[3,4] Therefore, calculations of electron affinities require systematic inclusion of both dynamic and nondynamic correlation.[5] At the same time, a highly diffused basis set, with maximum possible radical and angular flexibility,[6] is required to model the weakly bound electron, and it often makes the correlated calculations very time-consuming, sometimes impossible.

Among the various approaches available, the equation of motion coupled cluster (EOM-CC)[7,8] approach has been proved to be an accurate and systematic method for the calculation of electron affinities,[9−12] as a direct difference of energies. The EOM-CC approach for electron affinity (EOMEA-CC) is size-consistent, naturally spin adapted, and equivalent[13] to the (1, 0) sector of the Fock space multireference coupled cluster (FSMRCC)[14−17] method for the principal peaks. The EOMEA-CC method is generally used in singles and doubles approximations (EOMEA-CCSD). It scales as iterative N^6, and has similar storage requirements as that of the single-reference coupled cluster, which restrict its application beyond small molecules in moderate basis sets.

The single-reference coupled cluster theory has an intriguing relationship with many body perturbation theory.[18] Therefore, a natural way of approximating the coupled cluster effective Hamiltonian would be based on perturbation orders. Nooijen and Snijders[19] were the first to propose an approximation of the CCSD effective Hamiltonian by replacing the CCSD amplitudes with MBPT(2) amplitudes. Stanton and Gauss[20] generalized the approach by proposing a hierarchy of perturbative approximations to full EOM-CCSD, termed EOM-CCSD(n), where the effective Hamiltonian contains terms up to order n in perturbation. At a large value of n, EOM-CCSD(n) leads to full EOM-CCSD. The lowest order approximation to the EOM-CCSD(n) leads to EOM-CCSD(2) with MBPT(2) as ground state energy. The extension of this method to the ionization problem (EOMIP-CCSD(2)) leads to an N^5 scaling method with significantly less storage requirements than that of the standard EOMIP-CCSD method. Pal and co-workers[21] have recently shown that the EOMIP-CCSD(2) method can be used to study the geometry

Received: October 28, 2013
Published: April 1, 2014

   dx.doi.org/10.1021/ct4009409 | J. Chem. Theory Comput. 2014, 10, 1923−1933

and vibrational frequencies of large doublet radicals with accuracy comparable to that of the standard EOM-CCSD method. Ghosh and co-workers[22] have extended a similar idea in spin flip EOMCC and shown that the approximate effective Hamiltonian based EOMCC can be used for accurate description of potential energy surfaces.

The original implementation of EOM-CCSD(2) by Stanton and Gauss[20] was for the ionization problem (EOMIP-CCSD(2)) and excitation energy (EOMEE-CCSD(2)). The obvious extension of the EOM-CCSD(2) approach will be to the electron affinity problem. Recently, Jordan and co-workers[23,24] have used the EOMEA-CCSD(2) method to study electron attachment to water clusters and C60. The EOMEA-CCSD(2) method scales as N^5. However, unlike in the case of EOMIP-CCSD(2), the EOMEA-CCSD(2) has the same storage requirement as that of EOMEA-CCSD, which prohibits its usages beyond moderate size molecules. Bartlett and co-workers[25] have used a partitioned EOM matrix along with a MBPT(2) ground state, to reduce the scaling and storage requirement of the EOM-CCSD method for excitation energy. Taking inspiration from their work,[25−27] we have implemented a partitioning technique to the EOM based approach to the electron affinity problem, which leads to significant reduction in the storage requirements. Bartlett and co-workers[25] have used the name EOM-MBPT(2) for a second order approximation to the effective Hamiltonian. For the rest of the paper, we have followed the nomenclature of Bartlett and co-workers.[25]

The aim of this paper is to benchmark the comparative accuracy (relative to standard EOMEA-CCSD) of this new method (P-EOMEA-MBPT(2)) against the former EOMEA-MBPT(2) method and investigate its suitability to calculate electron affinities of large molecule and clusters. The paper is organized as follows. The next section contains the theory and implementation details of P-EOMEA-MBPT(2). Numerical results are discussed in section 3. Section 4 gives the concluding remarks.

2. THEORY AND IMPLEMENTATION DETAILS

a. EOMEA-CC. The equation of motion coupled cluster (EOM-CC) method[7] is a single-reference approach, where the excited state wave functions are generated by the action of a linear CI like operator on the correlated reference state wave function.

The Schrödinger equation for the reference state and the exited state (can be electron attached or ionized state also) can be described by

$$\hat{H}\Psi_0 = E_0\Psi_0 \tag{1}$$

$$\hat{H}\Psi_k = E_k\Psi_k \tag{2}$$

The excited state wave function Ψ_k is related to the reference state wave function by

$$\Psi_k = \hat{\Omega}_k\Psi_0 \tag{3}$$

Left multiplying eq 1 with $\hat{\Omega}_k$ and subtracting from eq 2, we get

$$[\hat{H}, \hat{\Omega}]\Psi_0 = \omega_k\Omega_k\Psi_0 \tag{4}$$

where $\omega_k = E_k - E_0$.

The form of Ω_k defines the particular EOM method corresponding to the target state.

For the electron affinity problem[9]

$$\Omega_k^{\mathrm{EA}} = \sum_a R^a(k)\hat{a}^\dagger + \sum_{a>b,j} R_j^{ab}(k)\hat{a}^\dagger\hat{j}\hat{b}^\dagger + \ldots \tag{5}$$

Coupled cluster theory is introduced by generating the correlated wave function by action of an exponential operator on a Slater determinant, which is generally, but not necessarily, a Hartree−Fock determinant.

$$\Psi_0 = e^{\hat{T}}|\Phi_0\rangle \tag{6}$$

where $\hat{T} = \hat{T}_1 + \hat{T}_2 + \ldots$ and $\hat{T}_1 = \sum_{ia} t_i^a\{a_a^\dagger a_i\}$, $\hat{T}_2 = 1/4\Sigma_{ijab} t_{ij}^{ab}\{a_a^\dagger a_b^\dagger a_j a_i\}$ ...

Since, $\hat{\Omega}$ and $\hat{T}$ commute among themselves, we can write eq 4 as

$$[\bar{H}, \hat{\Omega}]\Phi_0 = (\bar{H}\Omega)_c = \omega_k\hat{\Omega}_k\Phi_0 \tag{7}$$

where $\bar{H} = e^{-\hat{T}}He^{\hat{T}}$, and c denotes the connectedness of $\bar{H}$ and Ω.

Since $\bar{H}$ is non-Hermitian, there exist different right (R) and left (L) eigenvectors which are biorthogonal and can be normalized to satisfy

$$L_kR_l = \delta_{kl} \tag{8}$$

The method is equivalent to the (1,0) sector of the Fock space multireference coupled cluster (FSMRCC) method for the principal peaks.[13]

In a typical EOMEA-CCSD calculation, the electron affinities are obtained by diagonalization of the nonsymmetric effective Hamiltonian matrix in the $(N + 1)$ electron space

$$(\bar{H}) = \begin{bmatrix} \bar{H}_{\mathrm{SS}} & \bar{H}_{\mathrm{SD}} \\ \bar{H}_{\mathrm{DS}} & \bar{H}_{\mathrm{DD}} \end{bmatrix} \tag{9}$$

where $\bar{H}_{\mathrm{SS}}$ stands for the singles−singles block of the matrix and so on. The diagonalization is generally performed by the Davidson iterative technique.

The major step in the Davidson method is the multiplication of the matrix by trial vector R. In the case of EA, the equations for the multiplications are as follows (as described in ref 9)

$$[H_{\mathrm{SS}}R]^a = \sum_c F_{ac}R^c \tag{10}$$

$$[H_{\mathrm{SD}}R]^a = \sum_{id} F_{id}(2R_i^{ad} - R_i^{da}) + \sum_{cdi} R_i^{cd}(2W_{aicd} - W_{aidc}) \tag{11}$$

$$[H_{\mathrm{DS}}R]_j^{ab} = \sum_c W_{abcj}R^c \tag{12}$$

$$\begin{aligned}[H_{\mathrm{DD}}]_j^{ab} = {} & \sum_c F_{ac}R_j^{cb} + \sum_d F_{bd}R_j^{ad} - \sum_i F_{ij}R_j^{ab} \\ & + \sum_{id} (2W_{ibdj} - W_{bidj})R_i^{ad} - \sum_{ci} W_{aicj}R_i^{cb} \\ & - \sum_{ci} W_{bicj}R_i^{ca} + \sum_{cd} W_{abcd}R_j^{cd} \\ & - \sum_k \Big(\sum_{icd} [2V_{kicd} - V_{kidc}]R_i^{cd}\Big)t_{kj}^{ab}\end{aligned} \tag{13}$$

In the above equation, V denotes the normal mo integrals, and expressions for F and W intermediates are given in Appendix I.

b. EOMEA-MBPT(2). Approximating the coupled cluster amplitudes in eq 7 by MBPT(2) amplitudes leads to the

EOMEA-MBPT(2) method. It is an obvious extension of EOMIP-CCSD(2) and EOMEE-CCSD(2), by Stanton and Gauss,[20] to the electron affinity problem. The method can be trivially implemented by modifying the F and W intermediates in any standard EOMEA-CCSD code. The expressions for the modified F and W intermediates are given in Appendix 2.

The EOMEA-MBPT(2) scales as N^5 power of the basis set, but it has the same storage requirement as the normal EOMEA-CCSD. Especially, the computation of the W_{abcd} intermediate is the most time-consuming step in an EOMEA-MBPT(2) calculation and also the bottleneck of the method, which prohibits its applicability to large molecules.

Following Bartlett and co-worker's suggestion,[25] we propose a further approximation to the EOMEA-MBPT(2) method based on the partitioning of the EOM matrix.

c. P-EOMEA-MBPT(2). Following Löwdin's partitioning technique,[28] eq 7 can be partitioned into P and Q space, where P represents the principal configuration space and Q represents its orthogonal complement.

$$\begin{bmatrix} \bar{H}_{pp} & \bar{H}_{pq} \\ \bar{H}_{qp} & \bar{H}_{qq} \end{bmatrix} \begin{bmatrix} R_p \\ R_q \end{bmatrix} = \omega \begin{bmatrix} R_p \\ R_q \end{bmatrix} \tag{14}$$

and

$$[L_p \quad L_q] \begin{bmatrix} \bar{H}_{pp} & \bar{H}_{pq} \\ \bar{H}_{qp} & \bar{H}_{qq} \end{bmatrix} = [L_p \quad L_q]\omega \tag{15}$$

where R_p (L_p) and R_q (L_q) represent the projection of the right (left) eigenvector on P and Q spaces.

Expanding eq 14, we get

$$\bar{H}_{pp}R_p + \bar{H}_{pq}R_q = \omega R_p \tag{16}$$

$$\bar{H}_{qp}R_p + \bar{H}_{qq}R_q = \omega R_q \tag{17}$$

Rearranging eq 17

$$R_q = [\omega - \bar{H}_{qq}]^{-1}\bar{H}_{qp}R_p \tag{18}$$

Inserting R_q back into eq 16, we get

$$\bar{H}_{\text{eff}}R_p \equiv (\bar{H}_{pp} + \bar{H}_{pq}[\omega - \bar{H}_{qq}]^{-1}\bar{H}_{qp})R_p = \omega R_p \tag{19}$$

Projecting eq 19 with L_p

$$\begin{aligned} \langle L_p|\bar{H}_{\text{eff}}|R_p\rangle &\equiv \langle L_p|[\bar{H}_{pp} + \bar{H}_{pq}[\omega - \bar{H}_{qq}]^{-1}\bar{H}_{qp}]|R_p\rangle \\ &= \omega\langle L_p|R_p\rangle \end{aligned} \tag{20}$$

The eigenvalues of H_{eff} are solely defined in the P space, for the first several eigenvalues.

Now, if the exact eigenvalue ω is written as the sum of zeroth order energy ω_0, as of yet undetermined, and an energy correction $\Delta\omega$, we can write the operator inverse in eq 20 as

$$\begin{aligned} [\omega - \bar{H}_{qq}]^{-1} &= [\omega_0 + \Delta\omega - \bar{H}_{qq}^{[0]} - \bar{H}_{qq}^{[1]} - \bar{H}_{qq}^{[2]}...]^{-1} \\ &= [(\omega_0 - \bar{H}_{qq}^{[0]})(1 - [\omega_0 - \bar{H}_{qq}^{[0]}]^{-1} \\ &\quad [\bar{H}_{qq}^{[1]} + \bar{H}_{qq}^{[2]}... - \Delta\omega])]^{-1} \\ &\equiv [(\omega_0 - \bar{H}_{qq}^{[0]}) \\ &\quad (1 - [\omega_0 - \bar{H}_{qq}^{[0]}]^{-1}[V_{qq} - \Delta\omega])]^{-1} \end{aligned} \tag{21}$$

where $V_{qq} = \bar{H}_{qq}^{[1]} + \bar{H}_{qq}^{[2]} + ...$

Now eq 21 can be expanded in an inverse series

$$\begin{aligned} [\omega - \bar{H}_{qq}]^{-1} &= [\omega_0 - \bar{H}_{qq}^{[0]}]^{-1} + [\omega_0 - \bar{H}_{qq}^{[0]}]^{-1} \\ &\quad (V_{qq} - \Delta\omega)[\omega_0 - \bar{H}_{qq}^{[0]}]^{-1} \\ &\quad + [\omega_0 - \bar{H}_{qq}^{[0]}]^{-1}(V_{qq} - \Delta\omega)[\omega_0 - \bar{H}_{qq}^{[0]}]^{-1} \\ &\quad (V_{qq} - \Delta\omega)[\omega_0 - \bar{H}_{qq}^{[0]}]^{-1} + ... \end{aligned} \tag{22}$$

The lowest order approximation to eq 22 will be

$$[\omega - \bar{H}_{qq}]^{-1} \equiv [\omega_0 - \bar{H}_{qq}^{[0]}]^{-1} \tag{23}$$

where $\bar{H}_{qq}^{[0]}$ is the usual Møller−Plesset unperturbed Hamiltonian in Q space.

In other words, the unfolded matrix in eq 9 is approximated as

$$(\bar{H}) \equiv \begin{bmatrix} \bar{H}_{\text{SS}} & \bar{H}_{\text{SD}} \\ \bar{H}_{\text{DS}} & \bar{H}_{\text{DD}}^{[0]} \end{bmatrix} \tag{24}$$

and eq 13 becomes

$$[H_{\text{DD}}^{[0]}]_j^{ab} = \sum_c f_{ac}R_j^{cb} + \sum_d f_{bd}R_j^{ad} - \sum_i f_{ij}R_j^{ab} \tag{25}$$

Here, f is the Fock operator. In the case of RHF or UHF, reference $\bar{H}_{\text{DD}}^{[0]}$ becomes diagonal with the difference of orbital energy in the diagonal.

An examination of eqs 10−12 and eq 25 reveals that there is no four particle intermediate in the partition−EOMEA-CC (P-EOMEA) method. The four particle $\langle ab|cd\rangle$ integrals can indeed contract with T_1 amplitudes to contribute into the W_{abci} intermediate. However, an MBPT(2) ground state reference for the RHF or UHF case will lead to zero T_1 amplitudes. So P-EOMEA-MBPT(2) does not contain any four particle terms, which leads to a significant decrease in the storage requirements compared to the standard EOMEA-CCSD and EOMEA-MBPT(2). The P-EOMEA-MBPT(2) method is effectively N^5 scaling. A few N^6 scaling terms remain in $\bar{H}$, but these terms needed to be calculated only once. Alternatively, these terms can be calculated in an iterative N^5 scaling algorithm, following the approach presented in refs 7 and20. However, the results presented in this paper were calculated using the former approach.

Here, it should be noted that the H_{DD} block in the EOMEA matrix accounts for the electron attached states dominated by double-excitation character, i.e., states which are formed by the addition of an extra electron to the virtual orbitals of the reference state accompanied by excitation of the electron from the occupied to the virtual orbital. In the EOMEA-CCSD method, these doubly excited states are treated only in an approximate manner. It is well-known that the doubly excited determinant gives the major contribution in any correlation method. However, the R_2 operator in the EOMEA method can account for the only one electron excitations. On the other hand, the two electron excited determinants are accurately taken care of in the reference state by the T_2 amplitudes in the CCSD method. This leads to an imbalance in the description of the reference and the target state in the EOMEA-CCSD method and requires inclusion of triples, in both reference and target state calculations, for an accurate description of the electron attached state dominated by double excitations. In the partitioned EOMEA method, this H_{DD} block is further

dx.doi.org/10.1021/ct4009409 | J. Chem. Theory Comput. 2014, 10, 1923−1933

approximated to include only the diagonal terms. Therefore, the P-EOM based method is expected to give inferior performance for the states dominated by double excitations compared to the standard EOM method with an untruncated H_{DD} doubles−doubles block.

d. Size Consistency of P-EOMEA-MBPT(2). Size consistency is defined in the literature[29,30] as the additive separability of energy in the limit of noninteracting fragments.

$$E_{AB} = E_A + E_B \tag{26}$$

where E_{AB} is the energy of the system AB, consisting of two noninteracting fragments. E_A and E_B are individual energies of fragments A and B, respectively.

Now for the P-EOMEA-MBPT(2) to be size-consistent, the sum of the reference energy and the transition energy (electron attachment in this case) has to be size-consistent. Stanton and Gauss have shown that truncation of the effective Hamiltonian based on the perturbation orders will ensure size-consistency of the ground state energy for each order of perturbation. The detailed derivation is presented in ref 20.

Now for investigating the separability of the electron attachment energies, one needs to pay attention to the CI like linear operator Ω. Let us consider that the electron attachment is taking place on fragment A. The Hamiltonian of the system AB is the sum of the fragment A and B in the noninteracting limit

$$\hat{H}_{AB} = \hat{H}_A + \hat{H}_B \tag{27}$$

To ensure the additive separability of the energy, the Hamiltonian should be expressible in the block diagonal form.

$$\hat{H}_{AB} = \begin{pmatrix} H_{0,0} & H_{0,A} & H_{0,B} & H_{0,AB} \\ H_{A,0} & H_{A,A} & H_{A,B} & H_{A,AB} \\ H_{B,0} & H_{B,A} & H_{B,B} & H_{B,AB} \\ H_{AB,0} & H_{AB,A} & H_{AB,B} & H_{AB,AB} \end{pmatrix} \tag{28}$$

where $H_{AB,AB} = \langle \Psi_A \Psi_B | H_A + H_B | \Psi_A \Psi_B \rangle$, and so on. 0_A, 0_B, Ψ_A, and Ψ_B represent reference and electron attached states on A and B, respectively. Following refs 28 and 29, most of the terms in Hamiltonian $\hat{H}_{AB}$ can be shown to be zero. The reference state and the target state cannot be connected through the Hamiltonian, as they differ in spin multiplicity (singlet and doublet respectively). Therefore, the terms $H_{X,0}$ and $H_{0,X}$ are zero, where X = A, B, and AB. It should be noted that these terms are not necessarily zero for the excitation energy case.

Thus, $\hat{H}_{AB}$ simplifies to

$$\hat{H}_{AB} = \begin{pmatrix} H_{0,0} & 0 & 0 & 0 \\ 0 & H_{A,A} & H_{A,B} & H_{A,AB} \\ 0 & H_{B,A} & H_{B,B} & H_{B,AB} \\ 0 & H_{AB,A} & H_{AB,B} & H_{AB,AB} \end{pmatrix} \tag{29}$$

In the noninteracting limit, the $\hat{H}_A$ acts only on states of A and $\hat{H}_B$ acts only on states of B. Consequently, the terms H_{AB} and H_{BA} are zero.

$$\begin{aligned} H_{A,B} &= \langle \Psi_A 0_B | \hat{H}_A + \hat{H}_B | 0_A \Psi_B \rangle \\ &= \langle \Psi_A 0_B | \hat{H}_A | 0_A \Psi_B \rangle + \langle \Psi_A 0_B | \hat{H}_B | 0_A \Psi_B \rangle \\ &= \langle 0_B | \Psi_B \rangle \langle \Psi_A | \hat{H}_A | 0_A \rangle + \langle \Psi_A | 0_B \rangle \langle 0_B | \hat{H}_B | \Psi_B \rangle \\ &= 0 \langle \Psi_A | \hat{H}_A | 0_A \rangle + 0 \langle 0_B | \hat{H}_B | \Psi_B \rangle \\ &= 0 \end{aligned} \tag{30}$$

Now little attention has to be paid toward the term $H_{A,AB}$

$$\begin{aligned} H_{A,AB} &= \langle \Psi_A 0_B | \hat{H}_A + \hat{H}_B | \Psi_A \Psi_B \rangle \\ &= \langle 0_B | \Psi_B \rangle \langle \Psi_A | \hat{H}_A | \Psi_A \rangle + \langle \Psi_A | \Psi_A \rangle \langle 0_B | \hat{H}_B | \Psi_B \rangle \\ &= 0 + \langle \Psi_A | \Psi_A \rangle \langle 0_B | \hat{H}_B | \Psi_B \rangle \end{aligned} \tag{31}$$

The first term of eq 31 is trivially zero. Let us take the electron attachment takes place on fragment A. As the determinant Ψ_A includes at least one electron attachment, the excitation level in the determinant Ψ_B will be restricted to a maximum of single substitution. Thus, $\langle 0_B | \hat{H}_B | \Psi_B \rangle$ becomes zero due to Brillouin's theorem. Following the similar analogy, $H_{B,AB}$, $H_{AB,A}$, and $H_{AB,B}$ can also be shown to be zero. The proof is the same if the electron attachment takes place in fragment B.

All of the above conditions hold true, even for a partitioned form of the Hamiltonian

The target states are obtained by the diagonalization of $\hat{H}_{AB}$ and are, thus, defined by the following secular equation:

$$\begin{pmatrix} H_{0,0} - \omega I & 0 & 0 & 0 \\ 0 & H_{A,A} - \omega I & 0 & 0 \\ 0 & 0 & H_{B,B} - \omega I & 0 \\ 0 & 0 & 0 & H_{AB,AB} - \omega I \end{pmatrix} = 0 \tag{32}$$

where I stands for the unity matrix and ω is the corresponding eigenvalue.

Equation 32 is satisfied when

$$\begin{aligned} &|H_{0,0} - \omega I| \times |H_{A,A} - \omega I| \times |H_{B,B} - \omega I| \times |H_{AB,AB} - \omega I| \\ &= 0 \end{aligned} \tag{33}$$

which means the eigenvalues of the individual fragment are also the eigenvalue of the combined system.

Therefore, the transition energies in the P-EOMEA-MBPT(2) method are size-intensive.

Hence, the total energy, which is sum of the reference state energy and transition energies, is also size-consistent.

e. Computational Details. Vertical electron affinities are calculated for small molecules like N_2, H_2O, NO^+, O_3, and H_2CO using the P-EOMEA-MBPT(2) method, in a hierarchy of Dunning's correlation consistent aug-cc-pVXZ (X = D, T, Q) basis sets.[31] Experimental geometries are used in all of the cases. The results are compared with the standard EOMEA-CCSD, P-EOMEA-CCSD, and EOMEA-MBPT(2) methods.

After estimating the accuracy of the P-EOMEA-MBPT(2) method, we have used it to calculate the electron affinities of DNA and RNA nucleobases (NAB). We have calculated the electron affinities of adenine, guanine, thymine, cytosine, and uracil in the aug-cc-pVDZ and aug-cc-pVTZ basis sets, and the results are compared with the available experimental and theoretical values. Diffused f functions are removed from the aug-cc-pVTZ basis set, in the calculations for DNA nucleic acid

bases, to keep it computationally viable. All the calculations are performed using our in-house coupled cluster and EOMCC codes. Converged Hartree−Fock coefficients, eigenvectors, and one and two electron atomic integrals are taken from the GAMESS-US package.[32] All the calculations are performed assuming C_1 symmetry, and all the electron are used in correlation treatment.

3. RESULTS AND DISCUSSION

a. Benchmarking. The performance of the newly implemented P-EOMEA-MBPT(2) method is benchmarked for small molecules like N_2, H_2O, NO^+, O_3, and H_2CO in a hierarchy of Dunning's correlation consistent aug-cc-pVXZ (X = D, T, Q) basis set (Tables 1−5). For the sake of comparison, we also quote the corresponding P-EOMEA-CCSD and EOMEA-MBPT(2) results.

Table 1. Electron Affinities of N_2 (in eV)

basis	state	EOMEA-CCSD	P-EOMEA-CCSD	EOMEA-MBPT(2)	P-EOMEA-MBPT(2)
aug-cc-pVDZ	$^2\Sigma_u^-$	−2.64	−2.66	−2.64	−2.65
	$1\ ^2\Pi_g$	−2.69	−2.86	−2.68	−2.85
	$^2\Sigma_g^+$	−3.15	−3.18	−3.15	−3.18
	$^2\Pi_u$	−3.78	−3.80	−3.79	−3.80
aug-cc-pVTZ	$^2\Sigma_u^-$	−2.08	−2.07	−2.06	−2.07
	$^2\Sigma_g^+$	−2.26	−2.28	−2.26	−2.27
	$1\ ^2\Pi_g$	−2.46	−2.58	−2.43	−2.54
	$^2\Pi_u$	−2.94	−2.95	−2.94	−2.95
aug-cc-pVQZ	$^2\Sigma_u^-$	−1.70	−1.70	−1.69	−1.70
	$^2\Sigma_g^+$	−1.70	−1.71	−1.70	−1.71
	$1\ ^2\Pi_g$	−2.33	−2.41	−2.29	−2.37
	$^2\Pi_u$	−2.41	−2.41	−2.41	−2.41

Table 2. Electron Affinities of H_2O (in eV)

basis	state	EOMEA-CCSD	P-EOMEA-CCSD	EOMEA-MBPT(2)	P-EOMEA-MBPT(2)
	$1\ ^2A_1$	−0.78	−0.80	−0.77	−0.80
	$^2B_2$	−1.50	−1.51	−1.50	−1.52
aug-cc-pVDZ	$2\ ^2A_1$	−4.36	−4.40	−4.38	−4.43
	$3\ ^2A_1$	−5.17	−5.20	−5.20	−5.24
	$^2B_1$	−5.54	−5.61	−5.57	−5.64
	$1\ ^2A_1$	−0.62	−0.64	−0.63	−0.64
	$^2B_2$	−1.23	−1.24	−1.24	−1.24
aug-cc-pVTZ	$2\ ^2A_1$	−3.26	−3.28	−3.27	−3.30
	$3\ ^2A_1$	−4.04	−4.06	−4.06	−4.08
	$^2B_1$	−4.20	−4.24	−4.22	−4.26
	$1\ ^2A_1$	−0.54	−0.56	−0.55	−0.56
	$^2B2$	−1.10	−1.11	−1.11	−1.11
aug-cc-pVQZ	$2\ ^2A_1$	−2.70	−2.71	−2.71	−2.72
	$3\ ^2A_1$	−3.29	−3.30	−3.30	−3.32
	$^2B_1$	−3.45	−3.48	−3.45	−3.49

Table 1 presents the electron affinity values for first five states of N_2. It is well know that N_2^- is a temporary bound anion, which is evident from its negative electron affinity. It can be seen that all four methods give electron affinity values which are in good agreement with each other in all three basis sets, except for the $^2\Pi_g$ state, where both the P-EOM-CCSD and P-EOM-MBPT(2) underestimate the electron affinity value as compared to the EOM-CCSD and EOM-MBPT(2) methods, which are in good agreement with each other. Here it should be noted that the $^2\Pi_g$ state has significant double-excitation character, which is not properly taken care of by the partitioned EOM methods, due to a truncated doubles−doubles block of the EOM matrix. This leads to inferior performance of both the P-EOM-CCSD and P-EOM-MBPT(2) methods for the $^2\Pi_g$ state. The $^2\Sigma_u^-$, $^2\Sigma_g^+$, and $^2\Pi_u$ states, which are dominated by single excitation, are accurately reproduced by the partitioned methods. The increment of basis set from aug-cc-pVDZ to aug-cc-pVTZ leads to an increase in electron affinity for all the states. It also accompanies change in relative ordering of states. The $^2\Sigma_g^+$ state, which has been the fourth highest electron

Table 3. Electron Affinities of NO^+ (in eV)

basis	state	EOMEA-CCSD	P-EOMEA-CCSD	EOMEA-MBPT(2)	P-EOMEA-MBPT(2)
	X $^2\Pi$	9.38	9.25	9.39	9.25
	X $^2\Pi$	9.38	9.25	9.39	9.25
aug-cc-pVDZ	A $^2\Sigma^+$	3.33	3.31	3.31	3.29
	D $^2\Sigma^+$	2.10	2.10	2.14	2.12
	C $^2\Pi$	1.91	1.91	1.92	1.92
	X $^2\Pi$	9.65	9.59	9.66	9.60
	X $^2\Pi$	9.65	9.59	9.66	9.60
aug-cc-pVTZ	A $^2\Sigma^+$	3.52	3.51	3.51	3.50
	D $^2\Sigma^+$	2.39	2.39	2.41	2.40
	C $^2\Pi$	2.24	2.25	2.25	2.26
	X $^2\Pi$	9.74	9.72	9.77	9.74
	X $^2\Pi$	9.74	9.72	9.77	9.74
aug-cc-pVQZ	A $^2\Sigma^+$	3.65	3.65	3.65	3.65
	D $^2\Sigma^+$	2.54	2.54	2.55	2.55
	C $^2\Pi$	2.43	2.44	2.43	2.44

Table 4. Electron Affinities of O_3 (in eV)

basis	state	EOMEA-CCSD	P-EOMEA-CCSD	EOMEA-MBPT(2)	P-EOMEA-MBPT(2)
	$1\ ^2B_1$	1.62	1.58	1.18	1.16
	$^2B_2$	−3.05	−3.03	−3.09	−3.08
aug-cc-pVDZ	$1\ ^2A_1$	−3.07	−3.03	−3.10	−3.09
	$2\ ^2A_1$	−3.43	−3.41	−3.46	−3.46
	$2\ ^2B_1$	−4.47	−4.48	−4.53	−4.54
	$1\ ^2B_1$	1.84	1.88	1.42	1.49
	$^2B_2$	−2.47	−2.45	−2.50	−2.49
aug-cc-pVTZ	$1\ ^2A_1$	−2.55	−2.53	−2.55	−2.54
	$2\ ^2A_1$	−2.59	−2.55	−2.63	−2.60
	$2\ ^2B_1$	−3.49	−3.48	−3.52	−3.52
	$1\ ^2B_1$	1.94	2.03	1.53	1.65
	$^2B_2$	−1.91	−1.89	−1.92	−1.90
aug-cc-pVQZ	$1\ ^2A_1$	−2.01	−1.99	−2.03	−2.01
	$2\ ^2A_1$	−2.14	−2.12	−2.14	−2.13
	$2\ ^2B_1$	−2.85	−2.85	−2.88	−2.87

dx.doi.org/10.1021/ct4009409 | J. Chem. Theory Comput. 2014, 10, 1923−1933

Table 5. Electron Affinities of H_2CO (in eV)

basis	state	EOMEA-CCSD	P-EOMEA-CCSD	EOMEA-MBPT(2)	P-EOMEA-MBPT(2)
	1 $^2A_1$	−0.75	−0.77	−0.73	−0.75
	$^2B_2$	−1.25	−1.32	−1.24	−1.31
aug-cc-pVDZ	1 $^2B_1$	−1.31	−1.36	−1.29	−1.35
	2 $^2A_1$	−2.19	−2.22	−2.21	−2.24
	2 $^2B_1$	−3.10	−3.19	−3.08	−3.17
	1 $^2A_1$	−0.59	−0.60	−0.56	−0.58
	$^2B_2$	−1.07	−1.08	−1.05	−1.06
aug-cc-pVTZ	1 $^2B_1$	−1.08	−1.14	−1.05	−1.12
	2 $^2A_1$	−1.85	−1.87	−1.86	−1.88
	2 $^2B_1$	−2.48	−2.53	−2.44	−2.50
	1 $^2A_1$	−0.50	−0.50	−0.48	−0.49
	$^2B_2$	−0.96	−0.97	−0.95	−0.96
aug-cc-pVQZ	1 $^2B_1$	−0.99	−1.03	−0.96	−1.00
	2 $^2A_1$	−1.58	−1.59	−1.59	−1.60
	2 $^2B_1$	−2.11	−2.14	−2.07	−2.11

attached state, changes to the second highest electron attached state, on changing the basis from aug-cc-pVDZ to aug-cc-pVTZ. The discrepancy between the P-EOM vs EOM results, for the $^2\Pi_g$ states, slightly decreases in the aug-cc-pVTZ basis set. The electron affinity values of N_2 further increase from aug-cc-pVTZ to the aug-cc-pVQZ basis; however, the state ordering remains unchanged from that in the aug-cc-pVTZ basis set.

In Table 2, we report the electron affinity values for the first five states of water. Water also gives rise to a temporarily bound anion on electron attachment. The Hartree−Fock wave function provides a very good zeroth order description of the wave function of the ground state of water, as indicated by the small T1 diagnosis value. At the same time, the first five electron attached states are predominantly single-reference in nature. This leads to very good agreement of electron affinity values in all four methods, with each other, in all three basis sets. Incrementing in the basis set leads to an increase in electron affinity values for all five states in water.

Table 3 reports the electron affinity value for the five states of NO^+. The electron attachment to NO^+ is energetically favorable and, therefore, leads to positive values of electron affinities. We observe that the electron affinity values for the two $^2\Pi$ states is slightly underestimated in both P-EOM-CCSD and P-EOM-MBPT(2) methods. The slightly higher double excitation character for the $^2\Pi$ state is responsible for the discrepancy. The other three states, which are dominated by single excitation, are well described by the partitioned EOM methods. The electron affinity values for all five states increase with larger basis sets. The discrepancy between the P-EOM and EOM method for the $^2\Pi$ state also decreases in the aug-cc-pVTZ basis set. The electron affinity values for all five states further increase from aug-cc-pVTZ to the aug-cc-pVQZ basis, and in the aug-cc-pVQZ basis set, all the methods are in good agreement with each other.

The first five electron attached states of ozone are reported in Table 4. We observe that the electron affinity of the 1 $^2B_1$ state is positive, while the rest of the four states have negative electron affinity, which indicates that only the first state is stable upon electron attachment. The electron affinity values in all four methods increase with a better basis set. It can be seen that both the EOMEA-MBPT(2) as well as P-EOMEA-MBPT(2) methods significantly underestimate the electron affinity value for the 1 $^2B_1$ state, compared to the EOMEA-CCSD method. On the other hand, the electron affinity value for the 1 $^2B_1$ state in the P-EOMEA-CCSD method is in good agreement with the EOMEA-CCSD value for all three basis sets. Here, it should be noted that the presence of multireference character makes the restricted Hartree−Fock method wave function a poor choice for the correct zeroth order description for the ground state of ozone, which is indicated by the large T1 diagnosis values (see Table 6). In the case of both EOMEA-CCSD and P-EOMEA-CCSD methods, the T_1 amplitudes take care of the orbital relaxation. This is missing in both EOMEA-MBPT(2) and P-EOMEA-MBPT(2) methods and leads to the failure of both the methods for the 1 $^2B_1$ state. The picture in higher electron attached states is dominated by the large structural relaxation caused by the addition of an extra electron, which is properly taken care of by the EOM method. Therefore, both EOMEA-MBPT(2) and P-EOMEA-MBPT(2) give satisfactory performance for all of the higher electron attached states. The detailed analysis on the origin and the trends of the errors are presented in the next section.

Table 6. T1 Diagnosis Values in aug-cc-pVTZ Basis Set

molecule	T1 value
N_2	0.013
H_2O	0.010
NO^+	0.022
ozone	0.028
H_2CO	0.016

Electron affinity values for the five states of formaldehyde are presented in Table 5. The electron affinity values for all five states are negative, which indicates that the electron attachment to formaldehyde leads to temporary bound anions. The electron affinity values for all five states increase with incrementation in the basis set. All four methods show very good agreement with each other in all three basis sets.

As a passing remark, it should be mentioned that the calculated electron affinity values in all four methods have not converged with respect to basis set even in the aug-cc-pVQZ basis set. Therefore, it may be necessary to go for explicit correlation technique based[33] EOM methods to get the basis set convergence in the electron affinity values.

b. Error Analysis. To understand the trends and source of the errors in different approximations to the EOMEA-CCSD method, we have calculated the vertical electron affinities of 20 small molecules like N_2, H_2O, CH^+, F_2, C_2, CO, NH, NO^+, O_2, BH, O_3, C_2H_2, C_2H_4, CO_2, LIF, NaH, Cl_2, BeO, H_2S, and H_2CO, in a hierarchy of Dunning's correlation consistent aug-cc-pVXZ (X = D, T, Q) basis sets.[31] The detailed results are provided in the Supporting Information. The statistical analysis shows that the P-EOMEA-MBPT(2) method has an average absolute deviation (AAD) and root-mean-square deviation (RMSD) of 0.03 and 0.07 eV from the standard EOMEA-CCSD values (Table 7). The error bars are smaller than that in both P-EOMEA-CCSD and EOMEA-MBPT(2) methods. From Figure 1, it can be seen that the P-EOMEA-MBPT(2)

dx.doi.org/10.1021/ct4009409 | J. Chem. Theory Comput. 2014, 10, 1923−1933

Table 7. Maximum Absolute, Average Absolute, and Root Mean Square Deviation of Calculated Electron Affinity (in eV) from EOMEA-CCSD Values in the aug-cc-PVQZ Basis Set

method	P-EOMEA-CCSD	EOMEA-MBPT(2)	P-EOMEA-MBPT(2)
max abs dev	0.63	0.50	0.49
avr abs dev	0.04	0.05	0.03
RMS dev	0.10	0.11	0.07

method shows the least error in the electron affinity values among the three approximations to the standard EOMEA-CCSD method.

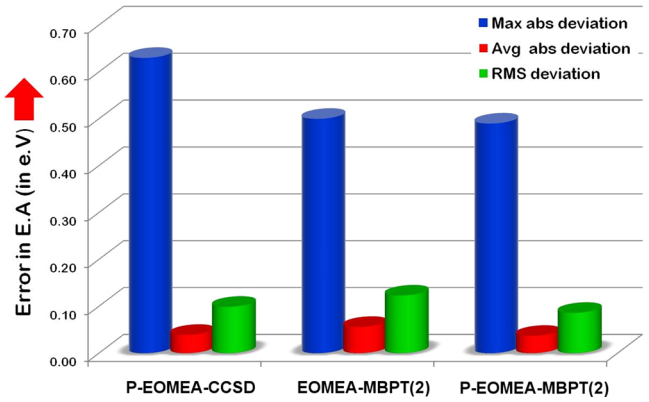

Figure 1. Maximum abs deviation, average abs deviation, and RMS deviation of different approximate EOMEA-CC methods from the full EOMEA-CCSD method (in eV).

Ghosh and co-workers[22] have shown that the use of EOM-MBPT(2) approximation leads to systematic underestimation of excitation energy in the spin-flip EOM method and proposed a linear relationship between the errors in reference and target state. However, in the case of the electron affinity problem, the correlation between error in the reference state and that in the target state will be less straightforward, as the reference and target states differ in the total number of electrons, unlike in the case of the excitation energy problem.

In general, the P-EOMEA-CCSD method overestimates and the EOMEA-MBPT(2) method underestimates the electron affinity values as compared to the standard EOMEA-CCSD method. However, the trends are less systematic. The truncated $\bar{H}_{DD}$ block of the partition EOMEA matrix leads to a rise in energy of the target state which in turn increases the energy difference between the reference and target states (if the target state is higher in energy than the reference state, see Figure 2), i.e., electron affinity value. This leads to systematic overestimation of electron affinity by the P-EOMEA-CCSD method.

In the case of the EOMEA-MBPT(2) method, the difference between E_{target}(EOMEA-CCSD) and E_{target}(EOMEA-MBPT(2)) is smaller than that in E_{ref}(CCSD) and E_{ref}(MBPT(2)), since the EOM operators R1 and R2 partly correct the error introduced due to the truncated T amplitudes. Thus, the electron affinity value ($E_{target} - E_{ref}$) calculated by the EOMEA-MBPT(2) method is lower than that calculated in the standard EOMEA-CCSD method. This leads to persistent underestimation of electron affinity values in the EOMEA-MBPT(2) method. In the P-EOMEA-MBPT(2) method, the

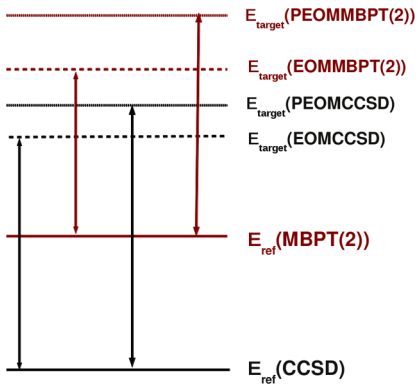

Figure 2. The error cancellation in the difference of energies between reference and target states.

truncated $\bar{H}_{DD}$ block reduces the power of the R_1 and R_2 operators to correct for the error in the target state, due to the truncated T amplitudes. This leads to a better balance in the errors in the E_{ref} and E_{target} states of the P-EOMEA-MBPT(2) method, resulting in systematic error cancelation to give a more accurate value of electron affinity ($E_{target} - E_{ref}$) values than that in the P-EOMEA-CCSD and EOMEA-MBPT(2) methods. However, the EOM vs P-EOM and the CCSD vs MBPT(2) errors are not exactly additive. The slightly higher error introduced by the P-EOM method in the target state compared to that caused by the MBPT(2) method in the reference state leads to underestimation of the electron affinity values in the P-EOMEA-MBPT(2) method. However, the magnitude of the errors in both the reference state and target state is small in most of the cases.

After gaining some confidence about the sufficient accuracy of the P-EOMEA-MBPT(2) method, we proceed to investigate the vertical electron affinities of DNA and RNA nucleic acid bases (NAB). The electron affinities of NAB are difficult to treat accurately with conventional *ab initio* methods, and NABs are too big to be investigated in the standard EOMEA-CCSD method, especially with modest computational resources.

C. Vertical Electron Affinities of DNA and RNA Nucleic Acid Bases. Accurate determination of electron affinities (EA) of DNA and RNA bases (Figure 3) plays a crucial role in understanding the electron donor and acceptor properties of NAB, such as charge transfer and charge transport along the DNA strand,[34] radiation damage and repair of the genetic material,[35] DNA protein interaction,[36] DNA phototherapy,[37] and DNA based molecular technologies.[38] A large number of experimental studies[39−46] has been performed for accurate determination of electron affinities. At the same time, numerous theoretical studies[47] with a wide range of theoretical methods, starting from DFT[48−51] to highly correlated CCSD-(T)[52,53] and CASPT2 methods,[52] have also been used for the elucidation of vertical and adiabatic electron affinities of NAB. Theoretical determination of EA of NAB is rather difficult, due to multiple reasons. The density functional theory (DFT) calculations show high dependence[47] on the exchange correlation functional. On the other hand, the state-of-the-art *ab initio* quantum mechanical calculations, although being more accurate, are difficult to perform due to the use of a highly diffused basis set, having the maximum radial and angular flexibility,[54] required to model the weakly bound electrons. The standard EOMEA-CCSD method, because of its systematic inclusion of dynamic and nondynamic correlation, is the ideal

dx.doi.org/10.1021/ct4009409 | J. Chem. Theory Comput. 2014, 10, 1923−1933

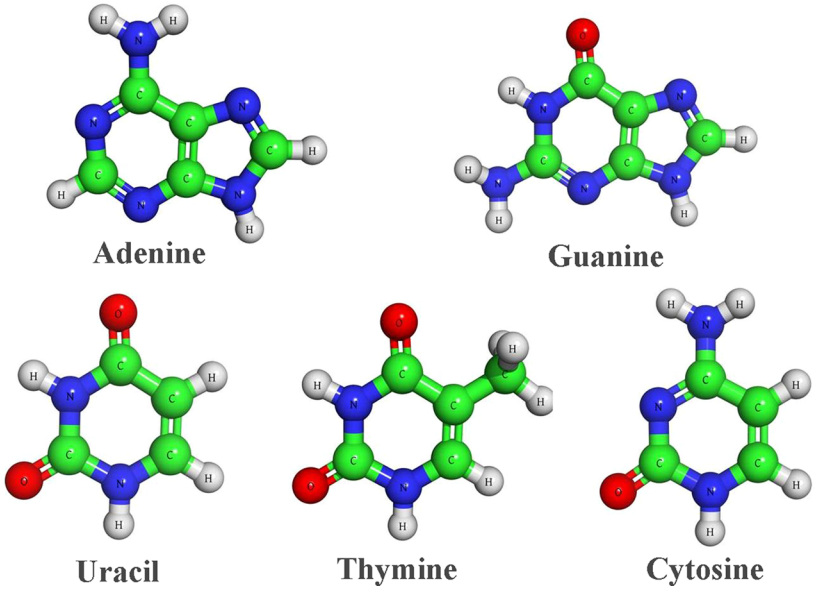

Figure 3. DNA and RNA Nucleic Acid Bases.

Table 8. Low-Lying Vertical Electron Affinities (eV) of DNA and RNA Nucleobases Obtained by Different Experimental, P-EOMEA-MBPT(2), and Other Theoretical Methods

method	uracil	thymine	cytosin	adenine	guanine
experimental range[a]	−0.30 to −0.22	−0.53 to −0.29	−0.55 to −0.32	−0.56 to −0.45	
exptl. (ETS)[b]	−0.22	−0.29	−0.32	−0.54	
scaled Koopman/D95 V[c]	−0.11	−0.32	−0.40	−0.74	−1.23
B3LYP range[d]	−1.09 to −0.11	−1.05 to −0.28	−1.42 to −0.31	−1.57 to −0.34	−2.07 to −0.08
MP2/6-31G(d)[e]	−1.77	−1.85	−1.97	−2.54	−2.82
PMP2//MP2/6-31G(d)[e]	−1.63	−1.69	−1.76	−2.07	−2.48
MP2/aug-cc-pVDZ	−0.69	−0.73	−0.91	−1.42	−1.57
PMP2//MP2/aug-cc-pVDZ[e]	−0.56	−0.58	−0.73	−0.99	−1.30
CCSD//CCSD/aug-cc-pVDZ[e]	−0.63	−0.65	−0.77		
CCSD(T)//CCSD/aug-cc-pVD[e]	−0.64	−0.65	−0.79		
CASPT2//CASSCF/cc-pVDZ[e]	−1.42	−1.44	−1.49	−1.65	−2.14
CASPT2//CASSCF/ANO-L 431/21[e]	−0.68	−0.69	−0.76	−1.06	−1.30
CASPT2/ANO-L 4321/321//CASSCF/ANO-L 431/21[e]	−0.49	−0.45	−0.59	−0.74	−0.94
P-EOMEA-MBPT(2)/aug-cc-pVDZ/B3LYP/aug-cc-pVTZ[f]	−0.17	−0.28	−0.46	−0.46	−0.34
P-EOMEA-MBPT(2)/aug-cc-pVTZ/B3LYP/aug-cc-pVTZ[f,g]	−0.14	−0.24	−0.41	−0.41	−0.30

[a]Values taken from refs 41−43. [b]Values taken from ref 41. [c]Values taken from ref 55. [d]Values taken from ref 47. [e]Values taken from ref 52. [f]Present work. [g]aug-cc-pVDZ basis used for hydrogen.

method for accurate theoretical estimations of EA of NAB. However, the prohibitively large computational cost has restricted the application of the EOMEA-CCSD method to NAB. To the best of our knowledge, no EOMCC study has been performed on electron affinities of NAB. The P-EOMEA-MBPT(2) method, because of its N^5 scaling and lesser storage requirements, can easily be applied to calculate the EA of NAB. Table 8 compiles the earlier reported theoretical results and present P-EOMEA-MBPT(2) values for the vertical EA of NAB, together with the available experimental data.

It can be seen that the experimental and theoretical methods provide negative vertical EA values for all the levels, which indicates that the NAB anions are temporary bound states or resonance states, existing in a short period of time and prone to autodetachment. An analysis of the theoretical methodologies employed for the calculation of vertical EA of NAB reveals that the DFT method gives the most scattered values, ranging from highly negative to nearly equal to zero, strongly dependent upon the functional and the quality of the basis set used. The simplest approach, i.e., via Koopman's approach[55] with some scale factor, gives values more or less similar to experimental values. The MP2 methods[52] lead to very high negative values in the 6-31G(d) basis set. However, the values become less negative with the use of diffused aug-cc-pVDZ. Spin contamination also has a significant effect on electron affinities calculated in the MP2 method. The use of the projected MP2 method makes the predicted electron affinity value less negative, i.e., closer to the experimental values. The CCSD-(T)[52] and CASPT(2)[52] give similar values, and both underestimate (i.e., gives more negative value) compared to the experimental results.

The P-EOMEA-MBPT(2) method gives the best agreement with the experimental values. There exists a striking difference in the trends of electron affinity values calculated in the P-EOMEA-MBPT(2) method with the earlier reported values. The electron affinities calculated using the P-EOMEA-

dx.doi.org/10.1021/ct4009409 | J. Chem. Theory Comput. 2014, 10, 1923−1933

MBPT(2) method are much less negative compared to that obtained in the MP2 and CCSD(T) method by Serrano-Andres and co-workers.[52] Especially the vertical EA for uracil is very small in the P-EOMEA-MBPT(2)/aug-cc-pVTZ level of theory, unlike that reported in the earlier theoretical investigation. It should be noted that the above CCSD(T) calculations by Serrano-Andres and co-workers[52] were performed in the small aug-cc-pVDZ basis set. The OVOS-CCSD(T) calculation in aug-cc-pVTZ by Urban and co-workers[53] has resulted in a vertical EA value of −0.15 eV for urcail, which is nearly identical with our P-EOMEA-MBPT(2) value of −0.14 eV. It is also interesting to note that the purine NAB, adenine and guanine, show significantly less negative values in P-EOMEA-MBPT(2) method than that in the CCSD(T) method.

The loosely bound electron in NAB anions may lead to multiple near-degenerate configurations requiring systematic inclusion of nondynamic correlation, which CCSD(T) fails to include in a balanced way. The electron affinity values calculated in the CASPT(2) method shows that with inclusion of nondynamic correlation, electron affinities become less negative. However, the CASPT(2) values strongly depend on the choice of active space. The EOM based methods, on the other hand, provide a balanced description of both dynamic and nondynamic correlation and is "black box" to use. Therefore, detailed studies of electron attachment and the electron attachment induced structural changes of NAB using EOMCC methods are required to get a better analysis of the experimental values. However, it is outside the scope of the present study and will be followed in a subsequent paper.

4. CONCLUSIONS

Electron attachment variant of EOM-CC offers a versatile approach to model electron attachment to atoms and molecules. In this work, we present an N^5 scaling, size-consistent modification to the standard EOMEA-CCSD method based on perturbation order analysis and the matrix partitioning technique. The proposed approximation (P-EOMEA-MBPT(2)) has significantly less storage than the earlier proposed EOMEA-MBPT(2) method. We have benchmarked the new method with standard EOMEA-CCSD methods. Statistical analysis of the results shows that P-EOMEA-MBPT(2) provides an inexpensive way for accurate determination of the electron affinities, when the ground state of the system is well described by the MBPT(1) wave function. For systems where the MBPT(1) wave function fails to properly describe the ground-state reference, no EOM-MBPT(2) method can give quantitatively accurate values and can only be used to get a mere qualitative picture. The P-EOMEA-MBPT(2) approximation gives similar accuracy to that of the previous EOMEA-MBPT(2) method, even better in most of the cases, in spite of the former having significantly lesser storage requirements. We have used the P-EOMEA-MBPT(2) method to calculate the electron affinities of DNA and RNA nucleic acid bases. The results have shown excellent agreement with experimental values.

The newly developed P-EOMEA-MBPT(2) method has immense potential to be used in the study of electron attachment to biological molecules and large clusters. The implementation of analytic derivatives is required for the purpose. Work is currently under way toward that direction.

APPENDIX I

Expressions for F and W intermediates for EOMEA-CCSD

$$F_{ij} = \sum_i F_i + \sum_{abk} (2t_{kj}^{ab} - t_{jk}^{ab} + 2t_k^a t_j^b - t_j^a t_k^b)\langle ki|ab\rangle + \sum_{ak} t_k^a (2\langle ik|ja\rangle - \langle ki|ja\rangle)$$

$$F_{ia} = \sum_{jb} t_j^b (2\langle ij|ab\rangle - \langle ij|ba\rangle)$$

$$F_{ab} = \sum_a f_a + \sum_{ijc} (-2t_{ji}^{ca} + t_{ij}^{ca} - 2t_j^c t_i^a + t_i^c t_j^a)\langle ji|bc\rangle + \sum_{ic} t_i^c (2\langle ai|bc\rangle - \langle ai|cb\rangle)$$

$$W_{aibj} = \langle ai|bj\rangle - \sum_{kc} (t_{ik}^{ba} + t_i^b t_k^a)\langle jk|bc\rangle - \sum_k t_k^a (\langle jk|ib\rangle - \langle ij|bk\rangle) + \sum_c t_i^c \langle aj|bc\rangle$$

$$W_{aijb} = \langle ai|jb\rangle + \sum_{kc} (2t_{ik}^{ac} - t_{ki}^{ac})\langle ik|bc\rangle - \sum_{ck} t_{ik}^{ac}\langle jk|cb\rangle + \sum_c t_i^c \langle aj|cb\rangle - \sum_k t_k^a \langle kj|ib\rangle - \sum_{kc} t_k^a t_i^c \langle kj|cb\rangle$$

$$W_{acbi} = \langle ac|bi\rangle + \sum_{lk} (t_{kl}^{bc} + t_k^b t_l^c)\langle lk|ia\rangle + \sum_{dk} (2t_{ki}^{dc} - t_{ik}^{dc} - t_i^d t_k^c)\langle da|bk\rangle - \sum_k t_k^b \langle ck|ia\rangle + \sum_b t_i^d \langle bc|ad\rangle - \sum_k t_k^c \langle kb|ia\rangle + \sum_{kld} t_{ki}^{dc} t_l^b \langle kl|ad\rangle + \sum_{kld} (t_{kl}^{cb} t_i^b + t_{li}^{bd} t_k^c)\langle kl|da\rangle - \sum_{kld} t_{il}^{cb} t_k^d (\langle kl|da\rangle - \langle lk|da\rangle) - \sum_{kd} (t_{ik}^{db} + t_i^d t_k^b)\langle ck|da\rangle - \sum_{kd} t_{ik}^{cd}\langle bk|da\rangle$$

$$W_{aibc} = \langle ai|bc\rangle - \sum_j t_j^b \langle ji|ca\rangle$$

$$W_{acbd} = \langle ac|bd\rangle + \sum_{kl} (t_{kl}^{ac} + t_k^a t_l^c)\langle kl|bd\rangle - \sum_k (t_k^a \langle ck|db\rangle + t_k^c \langle ak|bd\rangle)$$

APPENDIX II

Expressions for F and W intermediates for P-EOMEA-MBPT(2)

$$F_{ij} = \sum_i F_i + \sum_{abk} (2t_{kj}^{ab} - t_{jk}^{ab})\langle ki|ab\rangle$$

$$F_{ia} = 0$$

$$F_{ab} = \sum_a f_a + \sum_{ijc} (-2t_{ji}^{ca} + t_{ij}^{ca})\langle ji|bc\rangle$$

dx.doi.org/10.1021/ct4009409 | J. Chem. Theory Comput. 2014, 10, 1923−1933

$$W_{acbi} = \langle ac|bi\rangle + \sum_{lk} t_{kl}^{bc}\langle lk|ia\rangle + \sum_{dk}(2t_{ki}^{dc} - t_{ik}^{dc})\langle da|bk\rangle - \sum_{kd} t_{ik}^{db}\langle ck|da\rangle - \sum_{kd} t_{ik}^{cd}\langle bk|da\rangle$$

$$W_{aibc} = \langle ai|bc\rangle$$

■ ASSOCIATED CONTENT

Supporting Information

Cartesian coordinates the B3LYP/aug-cc-pVTZ optimized geometries, nuclear repulsion energy, SCF energy, correlation energy, and final energy of NABs and used experimental geometry and electron affinities of the test set molecules. This material is available free of charge via the Internet at http://pubs.acs.org.

■ AUTHOR INFORMATION

Corresponding Author

*E-mail: s.pal@ncl.res.in.

Notes

The authors declare no competing financial interest.

■ ACKNOWLEDGMENTS

The authors acknowledge the grant from CSIR XII[th] five year plan project on Multiscale Simulations of Material (MSM) and facilities of the Centre of Excellence in Scientific Computing at NCL. A.K.D thanks the Council of Scientific and Industrial Research (CSIR) for a Senior Research Fellowship. S.P. acknowledges the DST J. C. Bose Fellowship project and CSIR SSB grant towards completion of the work.

■ REFERENCES

(1) Crawford, O. H.; Garrett, W. R. Electron affinities of polar molecules. *J. Chem. Phys.* **1977**, *66*, 4968−4970.

(2) Desfrancois, C.; Abdoul-Carime, H.; Khelifa, N.; Schermann, J. P. From 1/r to $1/r^2$ Potentials: Electron Exchange between Rydberg Atoms and Polar Molecules. *Phys. Rev. Lett.* **1994**, *73*, 2436−2439.

(3) Sommerfeld, T.; DeFusco, A.; Jordan, K. D. Model Potential Approaches for Describing the Interaction of Excess Electrons with Water Clusters: Incorporation of Long-Range Correlation Effects. *J. Phys. Chem. A* **2008**, *112*, 11021−11035.

(4) Herbert, J. M.; Head-Gordon, M. Accuracy and limitations of second-order many-body perturbation theory for predicting vertical detachment energies of solvated-electron clusters. *Phys. Chem. Chem. Phys.* **2006**, *8*, 68−78.

(5) Hughes, S. R.; Kaldor, U. The Fock-space coupled-cluster method: Electron affinities of the five halogen elements with consideration of triple excitations. *J. Chem. Phys.* **1993**, *99*, 6773−6776.

(6) Raghavachari, K. Basis set and electron correlation effects on the electron affinities of first row atoms. *J. Chem. Phys.* **1985**, *82*, 4142−4146.

(7) Stanton, J. F.; Bartlett, R. J. The equation of motion coupled-cluster method. A systematic biorthogonal approach to molecular excitation energies, transition probabilities, and excited state properties. *J. Chem. Phys.* **1993**, *98*, 7029−7039.

(8) Krylov, A. I. Equation-of-Motion Coupled-Cluster Methods for Open-Shell and Electronically Excited Species: The Hitchhiker's Guide to Fock Space. *Annu. Rev. Phys. Chem.* **2008**, *59*, 433−462.

(9) Nooijen, M.; Bartlett, R. J. Equation of motion coupled cluster method for electron attachment. *J. Chem. Phys.* **1995**, *102*, 3629−3647.

(10) Nooijen, M.; Bartlett, R. J. Description of core-excitation spectra by the open-shell electron-attachment equation-of-motion coupled cluster method. *J. Chem. Phys.* **1995**, *102*, 6735−6756.

(11) Musial, M.; Bartlett, R. J. Equation-of-motion coupled cluster method with full inclusion of connected triple excitations for electron-attached states: EA-EOM-CCSDT. *J. Chem. Phys.* **2003**, *119*, 1901−1908.

(12) Gour, J. R.; Piecuch, P. Efficient formulation and computer implementation of the active-space electron-attached and ionized equation-of-motion coupled-cluster methods. *J. Chem. Phys.* **2006**, *125*, 234107−17.

(13) Musial, M.; Bartlett, R. J. Multireference Fock-space coupled-cluster and equation-of-motion coupled-cluster theories: The detailed interconnections. *J. Chem. Phys.* **2008**, *129*, 134105−12.

(14) Pal, S.; Rittby, M.; Bartlett, R. J.; Sinha, D.; Mukherjee, D. Molecular applications of multireference coupled-cluster methods using an incomplete model space: Direct calculation of excitation energies. *J. Chem. Phys.* **1988**, *88*, 4357−4366.

(15) Pal, S. Fock space multi-reference coupled-cluster method for energies and energy derivatives. *Mol. Phys.* **2010**, *108*, 3033−3042.

(16) Musial, M.; Bartlett, R. J. Intermediate Hamiltonian Fock-space multireference coupled-cluster method with full triples for calculation of excitation energies. *J. Chem. Phys.* **2008**, *129*, 044101−10.

(17) Kaldor, U.; Haque, A. Open-shell coupled-cluster method: Direct calculation of excitation energies. *Chem. Phys. Lett.* **1986**, *128*, 45−48.

(18) Bartlett, R. J. Many-Body Perturbation-Theory and Coupled Cluster Theory for Electron Correlation in Molecules. *Annu. Rev. Phys. Chem.* **1981**, *32*, 359−401.

(19) Nooijen, M.; Snijders, J. G. Second order many-body perturbation approximations to the coupled cluster Green's function. *J. Chem. Phys.* **1995**, *102*, 1681−1688.

(20) Stanton, J. F.; Gauss, J. Perturbative treatment of the similarity transformed Hamiltonian in equation-of-motion coupled-cluster approximations. *J. Chem. Phys.* **1995**, *103*, 1064−1076.

(21) Dutta, A. K.; Vaval, N.; Pal, S. Performance of the EOMIP-CCSD(2) Method for Determining the Structure and Properties of Doublet Radicals: A Benchmark Investigation. *J. Chem. Theory Comput.* **2013**, *9*, 4313−4331.

(22) Dutta, A. K.; Pal, S.; Ghosh, D. Perturbative approximations to single and double spin flip equation of motion coupled cluster singles doubles methods. *J. Chem. Phys.* **2013**, *139*, 124116−11.

(23) Voora, V. K.; Cederbaum, L. S.; Jordan, K. D. Existence of a Correlation Bound s-Type Anion State of C60. *J. Phys. Chem. Lett.* **2013**, *4*, 849−853.

(24) Vysotskiy, V. P.; Cederbaum, L. S.; Sommerfeld, T.; Voora, V. K.; Jordan, K. D. Benchmark Calculations of the Energies for Binding Excess Electrons to Water Clusters. *J. Chem. Theory Comput.* **2012**, *8*, 893−900.

(25) Gwaltney, S. R.; Nooijen, M.; Bartlett, R. J. Simplified methods for equation-of-motion coupled-cluster excited state calculations. *Chem. Phys. Lett.* **1996**, *248*, 189−198.

(26) Gwaltney, S. R.; Bartlett, R. J. Gradients for the partitioned equation-of-motion coupled-cluster method. *J. Chem. Phys.* **1999**, *110*, 62−71.

(27) Nooijen, M.; Ajith Perera, S.; Bartlett, R. J. Partitioned equation-of-motion coupled cluster approach to indirect nuclear spin-spin coupling constants. *Chem. Phys. Lett.* **1997**, *266*, 456−464.

(28) Löwdin, P.-O. Studies in perturbation theory: Part I. An elementary iteration-variation procedure for solving the Schrödinger equation by partitioning technique. *J. Mol. Spectrosc.* **1963**, *10*, 12−33.

(29) Krylov, A. I. Spin-flip configuration interaction: an electronic structure model that is both variational and size-consistent. *Chem. Phys. Lett.* **2001**, *350*, 522−530.

(30) Stanton, J. F. Separability properties of reduced and effective density matrices in the equation-of-motion coupled cluster method. *J. Chem. Phys.* **1994**, *101*, 8928−8937.

(31) Kendall, R. A.; Dunning, J. T. H.; Harrison, R. J. Electron affinities of the first-row atoms revisited. Systematic basis sets and wave functions. *J. Chem. Phys.* **1992**, *96*, 6796−6806.

(32) Schmidt, M. W.; Baldridge, K. K.; Boatz, J. A.; Elbert, S. T.; Gordon, M. S.; Jensen, J. H.; Koseki, S.; Matsunaga, N.; Nguyen, K. A.;

Su, S.; Windus, T. L.; Dupuis, M.; Montgomery, J. A. General atomic and molecular electronic structure system. *J. Comput. Chem.* **1993**, *14*, 1347−1363.
(33) Bokhan, D.; Ten-no, S. Communications: Explicitly correlated equation-of-motion coupled cluster method for ionized states. *J. Chem. Phys.* **2010**, *132*, 021101−4.
(34) Steenken, S. Purine bases, nucleosides, and nucleotides: aqueous solution redox chemistry and transformation reactions of their radical cations and e- and OH adducts. *Chem. Rev.* **1989**, *89*, 503−520.
(35) Colson, A.-O.; Sevilla, M. D. Structure and Relative Stability of Deoxyribose Radicals in a Model DNA Backbone: Ab Initio Molecular Orbital Calculations. *J. Phys. Chem.* **1995**, *99*, 3867−3874.
(36) Wintjens, R.; Lièvin, J.; Rooman, M.; Buisine, E. Contribution of cation-π interactions to the stability of protein-DNA complexes. *J. Mol. Biol.* **2000**, *302*, 393−408.
(37) Bonnett, R. *Chemical Aspects of Photodynamic Therapy*; CRC Press: Boca Raton, FL, 2000.
(38) Prasad, P. N. *Introduction to Biophotonics*; John Wiley & Sons: Hoboken, NJ, 2004.
(39) Wiley, J. R.; Robinson, J. M.; Ehdaie, S.; Chen, E. C. M.; Chen, E. S. D.; Wentworth, W. E. The determination of absolute electron affinities of the purines and pyrimidines in DNA and RNA from reversible reduction potentials. Biochem. *Biophys. Res. Commun.* **1991**, *180*, 841−845.
(40) Chen, E. C. M.; Wiley, J. R.; Batten, C. F.; Wentworth, W. E. Determination of the electron affinities of molecules using negative ion mass spectrometry. *J. Phys. Chem.* **1994**, *98*, 88−94.
(41) Aflatooni, K.; Gallup, G. A.; Burrow, P. D. Electron Attachment Energies of the DNA Bases. *J. Phys. Chem. A* **1998**, *102*, 6205−6207.
(42) Periquet, V.; Moreau, A.; Carles, S.; Schermann, J. P.; Desfrancois, C. Cluster size effects upon anion solvation of N-heterocyclic molecules and nucleic acid bases. *J. Electron Spectrosc. Relat. Phenom.* **2000**, *106*, 141−151.
(43) Haripriya, S.; Sangaranarayanan, M. V. Estimation of the electron affinities of nucleobases using thermochemical data and structural considerations. *J. Mol. Struct.* **2003**, *644*, 133−138.
(44) Chen, E. C. M.; Chen, E. S. Negative Ion Mass Spectra, Electron Affinities, Gas Phase Acidities, Bond Dissociation Energies, and Negative Ion States of Cytosine and Thymine. *J. Phys. Chem. B* **2000**, *104*, 7835−7844.
(45) Desfrancois, C.; Periquet, V.; Bouteiller, Y.; Schermann, J. P. Valence and Dipole Binding of Electrons to Uracil. *J. Phys. Chem. A* **1998**, *102*, 1274−1278.
(46) Compton, R. N.; Carman, J. H. S.; Desfrancois, C.; Abdoul-Carime, H.; Schermann, J. P.; Hendricks, J. H.; Lyapustina, S. A.; Bowen, K. H. On the binding of electrons to nitromethane: Dipole and valence bound anions. *J. Chem. Phys.* **1996**, *105*, 3472−3478.
(47) Gu, J.; Leszczynski, J.; Schaefer, H. F. Interactions of Electrons with Bare and Hydrated Biomolecules: From Nucleic Acid Bases to DNA Segments. *Chem. Rev.* **2012**, *112*, 5603−5640.
(48) Wetmore, S. D.; Boyd, R. J.; Eriksson, L. A. Theoretical Investigation of Adenine Radicals Generated in Irradiated DNA Components. *J. Phys. Chem. B* **1998**, *102*, 10602−10614.
(49) Richardson, N. A.; Wesolowski, S. S.; Schaefer, H. F. The Adenine-Thymine Base Pair Radical Anion: Adding an Electron Results in a Major Structural Change. *J. Phys. Chem. B* **2002**, *107*, 848−853.
(50) Gu, J.; Xie, Y.; Schaefer, H. F. Understanding Electron Attachment to the DNA Double Helix: The Thymidine Monophosphate-Adenine Pair in the Gas Phase and Aqueous Solution. *J. Phys. Chem. B* **2006**, *110*, 19696−19703.
(51) Richardson, N. A.; Wesolowski, S. S.; Schaefer, H. F. Electron Affinity of the Guanine-Cytosine Base Pair and Structural Perturbations upon Anion Formation. *J. Am. Chem. Soc.* **2002**, *124*, 10163−10170.
(52) Roca-Sanjuan, D.; Merchan, M.; Serrano-Andres, L.; Rubio, M. Ab initio determination of the electron affinities of DNA and RNA nucleobases. *J. Chem. Phys.* **2008**, *129*, 095104−11.
(53) Dedíková, P.; Demovíc, L.; Pitoňák, M.; Neogrády, P.; Urban, M. CCSD(T) calculations of the electron affinity of the uracil molecule. *Chem. Phys. Lett.* **2009**, *481*, 107−111.
(54) Rienstra-Kiracofe, J. C.; Tschumper, G. S.; Schaefer, H. F.; Nandi, S.; Ellison, G. B. Atomic and molecular electron affinities: photoelectron experiments and theoretical computations. *Chem. Rev.* **2002**, *102*, 231−282.
(55) Sevilla, M. D.; Besler, B.; Colson, A.-O. Ab Initio Molecular Orbital Calculations of DNA Radical Ions. 5. Scaling of Calculated Electron Affinities and Ionization Potentials to Experimental Values. *J. Phys. Chem.* **1995**, *99*, 1060−1063.